

A Simple Analytical Relationship between WM Tissue Characteristics and DWI Signal

S. Peled¹

¹Brigham and Women's Hospital, Boston, MA, United States

The major problem with quantitative DWI analysis for probing tissue microstructure is that crossing, fanning, and interleaving white matter tracts within voxels contribute to the signal, *mixing the cell-related information with orientation-related information*. For example, low anisotropy may indicate a disruption of intact axonal morphology, but may also be purely the result of a distribution of tract directions within a voxel. Although methods of untangling crossing tracts have started to emerge for tractography, they may never describe the tract configuration in a way that will allow complete separation of the orientation and the cellular information.

Here, with the help of a realistic, multi-*b*-value model of WM signal obtained in a few minutes from a *clinical scanner*, an analytical description of the DWI signal is presented that depends on tissue properties, such as extracellular signal fraction, intrinsic diffusion coefficient, and extracellular tortuosity. Through *summing* the different multi-*b*-value signals we eliminate the dependence on the exact tract directions that may exist within a voxel and retain relevant microstructural information – see below.

The Tensor-Stick Model

The main assumption of this model is that the intra-axonal water is restricted and exchange is slow on the timescale of the experiment. It follows from this that due to the long gradient pulses of clinical DWI scans ($\delta > 30$ ms), and the small size of axons, this water population experiences minimal signal attenuation when gradients are applied perpendicular to the long axis of the axon [Mitra95]. The apparent direction-dependent intracellular (IC) diffusion can thus be approximated as a “stick”: $D_{IC}(\theta) = D \cos^2 \theta$ where θ is the angle between the axon axis and the diffusion gradient direction, and D is the free diffusion constant inside the axon.

The 2nd assumption is that in clinical DWI scans, with typical TE's longer than 80ms, myelin associated water does not contribute significantly to the signal due to its short T_2 . Thus it is assumed the only other contribution to the signal is from the extracellular (EC) water which can be described as a tensor with 3 eigenvalues: $\{D, D_{\perp}, D_{\perp}\}$, or as an angle-dependent diffusion coefficient: $D_{EC}(\theta) = D \cos^2 \theta + D_{\perp} \sin^2 \theta$ where $D_{\perp} = D/\lambda^2$, and λ is the tortuosity. A similar approach has been utilized recently in Ref. [Fieremans2010]. According to this model, the *mean* signal after the application of N gradient directions (oriented in direction θ_j relative to the bundle axis), from a coherently oriented bundle of fibers is then:

$$S = \frac{1}{N} S_0 \sum_{j=1}^N \left[\alpha e^{-bD_{EC}(\theta_j)} + (1 - \alpha) e^{-bD_{IC}(\theta_j)} \right] \quad [1] \quad \text{where } S_0 \text{ is the signal at } b=0 \text{ and } \alpha \text{ is the signal fraction from the extracellular space.}$$

Eq.1 can be approximated as an integral: $S = \frac{1}{2} S_0 \int_0^{\pi} \left[\alpha e^{-bD_{EC}(\theta)} + (1 - \alpha) e^{-bD_{IC}(\theta)} \right] \sin \theta d\theta$ for

$$\text{which the exact solution is: } S = S_0 \frac{\sqrt{\pi}}{2} \left[\alpha e^{-bD_{\perp}} \frac{\text{erf}\left(\sqrt{b(D-D_{\perp})}\right)}{\sqrt{b(D-D_{\perp})}} + \frac{(1-\alpha) \text{erf}(\sqrt{bD})}{\sqrt{bD}} \right] \quad [2].$$

Fig. 1 shows a plot of Eq. 2 for $\alpha=[0.1,0.2,\dots,0.9]$ and *b*-values up to 3000 s/mm²; with an inset log-linear plot of the same data.

How Many Gradient Directions are Needed for Eq. 2 to be a good approximation of Eq. 1?

Very few - Fig. 2 shows the curve for Eq. 2 with $\alpha=0.5$, $D=2 \mu^2/\text{ms}$, and $\lambda=1.6$ in black, with red curves showing the upper and lower limits containing 90% of the results of applying Eq. 1 to gradient sets with 12 directions.

Directional Invariance: The tract-direction-invariance stems from the implicit assumption that the environment of each diffusing particle, insofar as that particle “senses” it, is a coherently directed structure, i.e, the extent of diffusion of a single particle does not encompass more than one tract direction. This means that the interleaving is rather coarse in crossing interleaved fibers, and sets a limit on the curvature of fanning fibers. Since the signals are summed from all gradient directions (and the sum of a sum is a sum!), within these loose constraints, *whatever the tract configuration inside the voxel, the above equations hold.*

Experiment: A healthy volunteer was scanned on a Siemens Trio 3T with 12 diffusion directions and 8 *b*-values. TE/TR=114/7500 ms, 45 slices, 3mm; matrix 128x128, FOV 25.6cm. Fig. 3 shows plots of Eq. 1 from 5 WM ROI's: corpus callosum genu (CCG), corpus callosum splenium (CCS), posterior internal capsule (PIC), frontal WM (FWM), and posterior WM (PWM).

The curves from heterogeneous WM (FWM & PWM) are similar to each other, as are the two curves from the corpus callosum, while the internal capsule curve is dissimilar to the others. Further analysis is beyond the scope of this abstract, which presents the analytical description and proof of its information content, but various methods of analysis are possible, and they do not necessarily require acquisition of many *b*-values.

Conclusion: Although there is a loss of information involved in summing all the diffusion curves, the resulting lack of dependence on (unknown) tract orientations has great value for the quantification of subtle changes in WM in every voxel. The description here results in an analytical expression for the multi-*b*-value diffusion signal from clinical scanners, that depends on tissue microstructural parameters.

References: [Mitra95] PP Mitra & BI Halperin. *J Mag Reson A*, **113**, p.94 (1995). [Fieremans2010] Fieremans E, Novikov DS, Jensen JH, Helpen JA. *NMR Biomed* **23**,p.711 (2010).

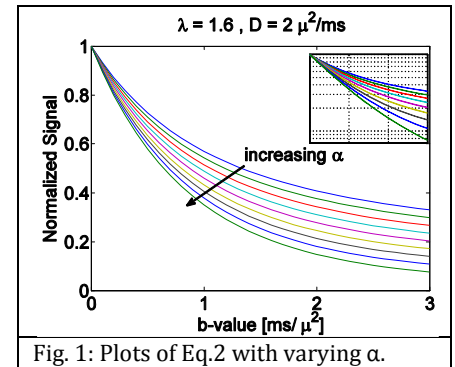


Fig. 1: Plots of Eq.2 with varying α .

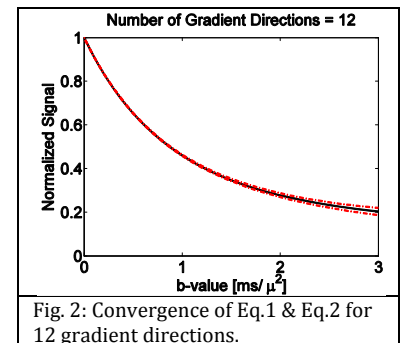


Fig. 2: Convergence of Eq.1 & Eq.2 for 12 gradient directions.

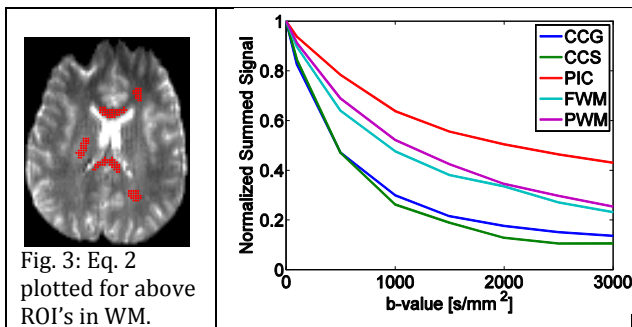


Fig. 3: Eq. 2 plotted for above ROI's in WM.